

## Supporting Information

### Tuning ice nucleation with pH-modulated Fe<sup>3+</sup> cross-linked hydrogel surfaces

Xiao Meng,<sup>a</sup> Yunhe Diao,<sup>a</sup> Ranran Zhu,<sup>a</sup> Fan Zhang,<sup>a</sup> Xuying Liu,<sup>a</sup> Jinzhou Chen,<sup>a</sup> and Huige Yang <sup>\*a</sup>

<sup>a</sup> School of Materials Science and Engineering, Zhengzhou University, Zhengzhou 450001, China.

\*Corresponding author.

E-mail: yanghg@zzu.edu.cn

### Experimental section

#### 1. Materials

Sodium alginate (SA, 200 ± 20 mPas), 1-(3-dimethylaminopropyl)-3-ethylcarbodiimide hydrochloride (EDC, 98%), and ferric chloride hexahydrate (FeCl<sub>3</sub>, 98%) were purchased from Aladdin (China). *N*-hydroxysuccinimide (NHS, 98+%) and Dopamine hydrochloride (DA, 99%) were purchased from Alfa Aesar (China). Phosphate buffered saline (PBS, 0.01M) was purchased from Solarbio (China). Dialysis membranes (molecular weight cutoff (MWCO)=3500 Da) were obtained from LABSEE (China). All the chemicals were of analytical grade and were not purified before use.

#### 2. Synthesis of Catechol-modified SA (SA-g-DA)

A carbodiimide coupling reaction was conducted for synthesizing the catechol-modified sodium alginate (SA-g-DA). Briefly, SA (324 mg) was dissolved in 30 mL of PBS buffer, and the pH of the system was adjusted to 5 using HCl (1 M). Subsequently, EDC (863 mg) and NHS (518 mg) were added to the mixture sequentially. The mixture was stirred for half an hour to dissolve completely. Next, DA (853 mg) was added to the mixture, maintaining a pH of 5, stirring overnight under an atmosphere of nitrogen. The molar ratio of the reactants was SA:EDC:NHS:DA=1:3:3:3. Then, the solution was transferred to a dialysis membrane (MWCO=3500) and dialyzed in an aqueous solution with pH=5.0 adjusted by 1M HCl for 2d, and the solution was dialyzed again in ultrapure water for 1 d to remove unreacted reagents and salts. The final product SA-g-DA was freeze-dried and stored at 4 °C.

#### 3. Fabrication of SA-g-DA/Fe<sup>3+</sup> Hydrogel Surface

The SA-g-DA conjugate was completely dissolved in 3000  $\mu\text{L}$  of PBS buffer at 1% (w/v), and then 540  $\mu\text{L}$   $\text{FeCl}_3$  solution (concentration: 25 mM) was added (the molar ratio of DOPA to  $\text{Fe}^{3+}$  is 3:1), and uniformly mixed. Then, the pH value of the solution was adjusted using 1 M HCl or 1 M NaOH for coordination crosslinking to form a hydrogel, and the gel was physically mixed until a uniform color and physical state were established. We prepared samples at final pH values of 3, 5, 7, 9, and 11, respectively. The pH of the hydrogels was measured using a pH meter (METTLER TOLEDO).

The silicon wafers (7 mm x 7 mm) were ultrasonically cleaned in acetone, isopropanol, anhydrous ethanol, and ultrapure water for 20 min. Following this, it was dried under a flow of nitrogen gas. The samples were immersed in the gel samples and removed after 6 h. The samples were rinsed with ultrapure water to remove the excess material on the surface and finally dried under a flow of high-purity nitrogen gas to obtain the hydrogel surface.

#### **4. Characterization**

We used the Fourier transform infrared spectroscopy (FT-IR, Bruker, Tensor II) and Nuclear magnetic resonance spectroscopy (NMR, Bruker, AV III HD) techniques to test the structure of the SA-g-DA conjugates. The degree of crosslinking of hydrogels with different pH was analyzed using the UV-Vis spectroscopy technique (Agilent Cary 5000). Water content of hydrogels determined by weighing method. A drop size analyzer (DataPhysics, OCA 40) was used to characterize the static contact angle of the substrate and the wettability of the hydrogel surface at different pH. The surface morphology and elemental composition of the hydrogel surface were studied using atomic force microscopy (AFM, Bruker, JPK BIOAFM, Icon). 3D surface profiler (QUESTAR, S lynx) was used to determine the film thicknesses of the hydrogel surface at different pH values. X-ray photoelectron spectroscopy (XPS, Thermo Fisher Scientific K-alpha) techniques. In addition, the differential scanning calorimetry (DSC, SHK, DSC 60) technique was used to obtain the freezing and melting information of the freezing bound water and bulk-like water in hydrogels with varying crosslinking degrees.

#### **5. Measurement of the Ice Nucleation Temperature and Delay Time**

We performed the experiments in a clean room. Three ultrapure water droplets (0.1  $\mu\text{L}$ ) were dispersed on the gel-modified surface to avoid freezing caused by the mutual influence of the water droplets. The droplets were taken in a self-made closed chamber and cooled with a cryostage at the rates of 2  $^\circ\text{C min}^{-1}$ , 5  $^\circ\text{C min}^{-1}$ , 10  $^\circ\text{C min}^{-1}$ , and 15  $^\circ\text{C min}^{-1}$  to gradually reduce the surface temperature of the sample to induce ice nucleation. To be

clear, the time which was taken by the water droplet from the initiation of ice nucleation in it to complete freezing ( $t_f$ ) is often short (usually tens of milliseconds for the droplet sizes investigated in this work), and thus the freezing of the entire droplet can be negligibly minute regarding the involved cooling rates. Besides, the  $t_f$  comparatively short relative to the delay time of ice nucleation (the period covering the time taken to reach the target temperature on the surface to the initiation of ice nucleation). As a result, the sudden change in opacity can detect the ice nucleation temperature ( $T_h$ ) and the delay time of ice nucleation ( $t_d$ ) within the cooling process of water droplets. A polarizing microscope was used for observation. The temperature of ice nucleation was recorded. The freezing tests were repeated 150 times to obtain reliable ice nucleation temperature statistics.

Likewise, to ensure that the experiments were performed in a closed environment at a constant relative humidity of 100%, the delay time of ice nucleation was tested within a chamber. The surface temperature was lowered to the target temperature (-26 °C), and this temperature was maintained until the water droplets froze. The time for which the water droplets remained unfrozen at the target temperature was defined as the delay time of ice nucleation ( $t_d$ ).

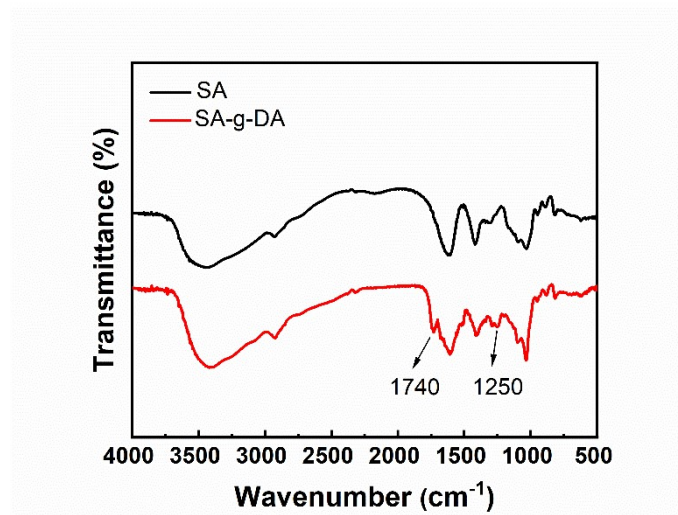


**Fig. S1** FT-IR spectra of SA and SA-g-DA conjugate.

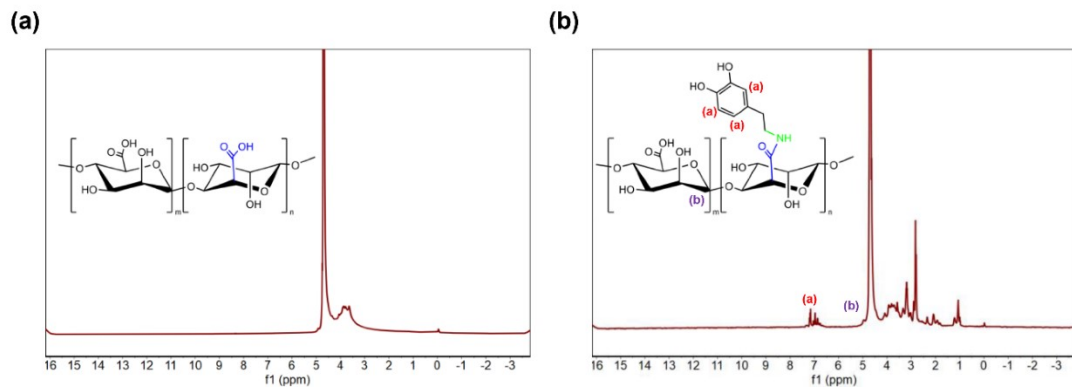


**Fig. S2**  $^1\text{H-NMR}$  spectra of (a) SA and (b) SA-g-DA conjugate.

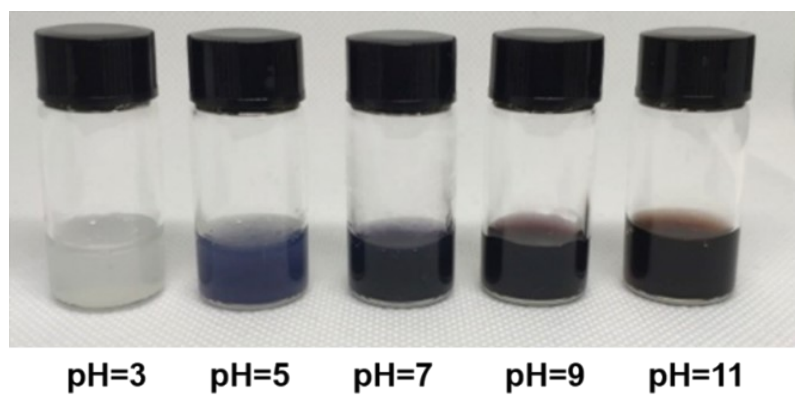


**Fig. S3** Hydrogels at different pH conditions show different colors.

**Table S1.** Water content of hydrogels at different pH.

pH value	Water content
3	85.5%
5	79.4%
7	75.8%
9	70.5%
11	62.4%

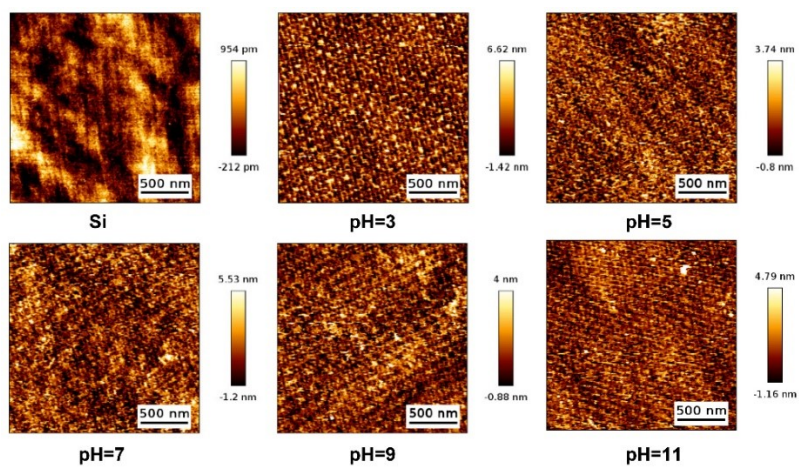


**Fig. S4** AFM images of silicon wafer and hydrogel surfaces at different pH conditions ( $2 \mu\text{m} \times 2 \mu\text{m}$ ).



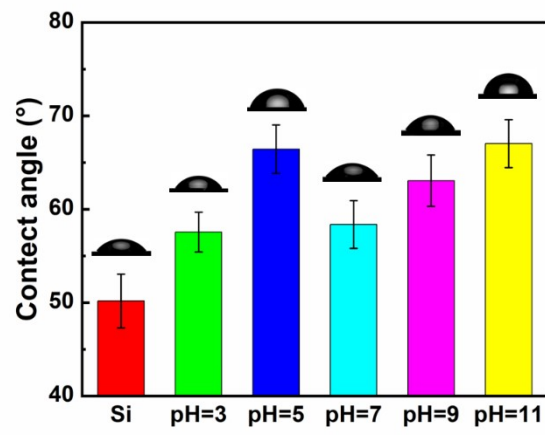


**Fig. S5** Static contact angles of silicon wafer and hydrogel surfaces at different pH conditions.

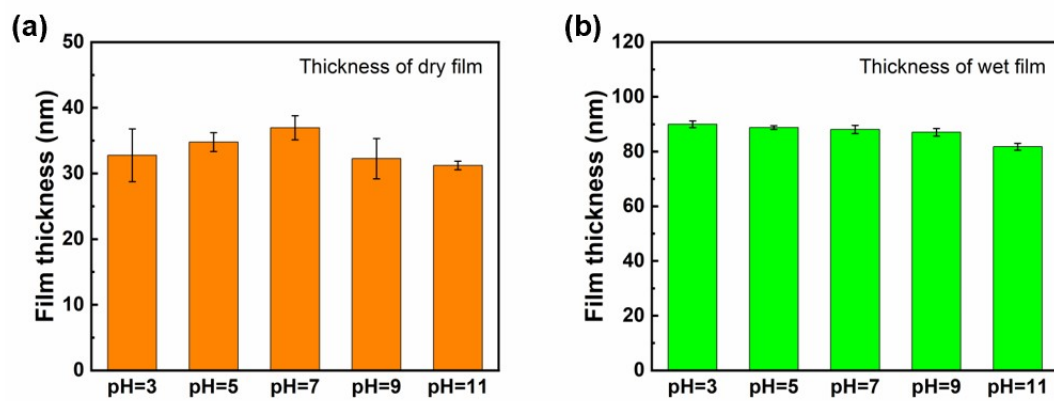


**Fig. S6** (a) Dry and (b) wet film thicknesses of hydrogel-modified surfaces at different pH conditions.

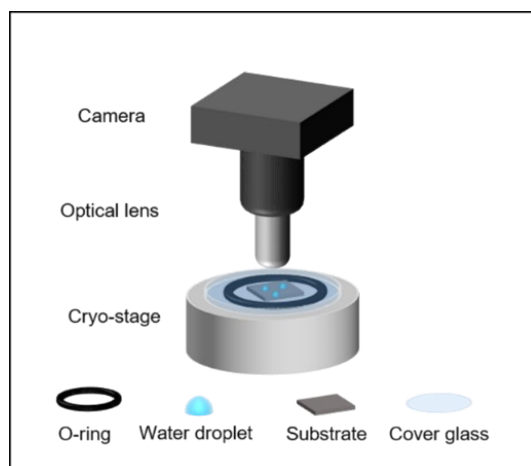


**Fig. S7** Schematic diagram of the device used for measuring surface ice nucleation temperature and delay time.

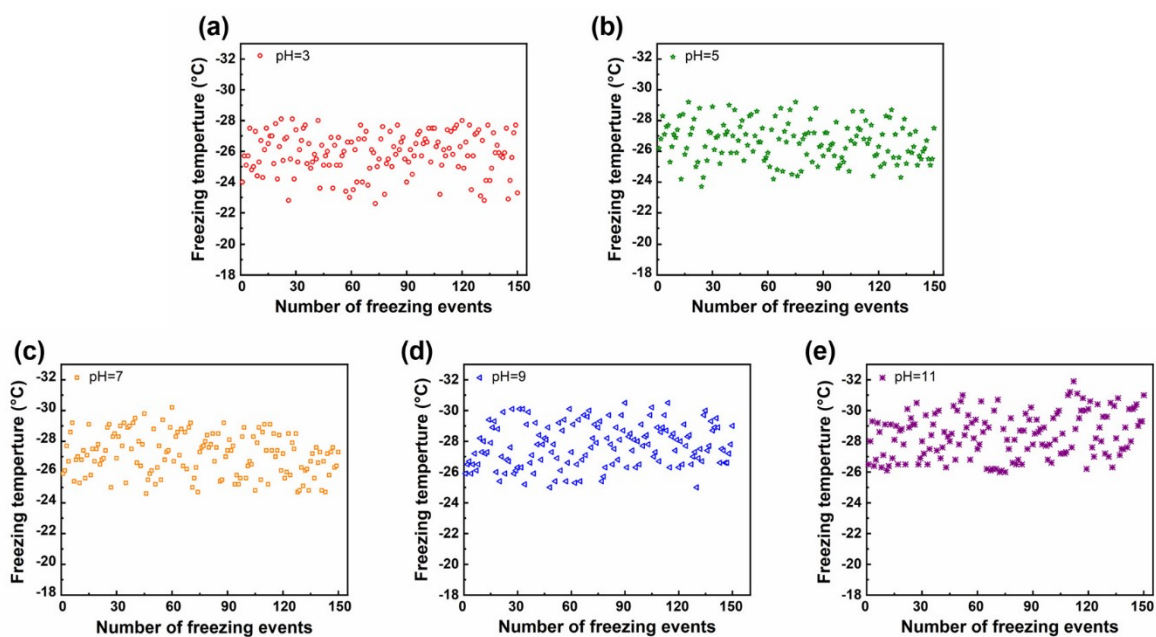


**Fig. S8** Freezing temperature as a function of freezing events for hydrogel-modified surfaces at different pH conditions obtained at the cooling rate of  $2\text{ }^{\circ}\text{C min}^{-1}$ , respectively.

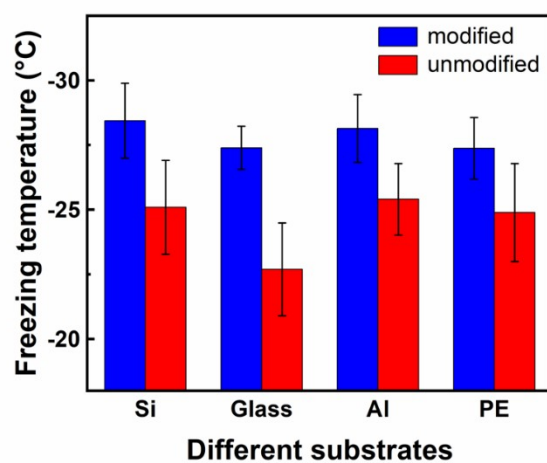


**Fig. S9** Ice nucleation temperature on a wide range of substrates before and after modified by hydrogels at pH=11 (2 °C min<sup>-1</sup>)

**Table S2.** DSC data.

pH value	$T_{f,b}$ (°C)	$\Delta H_{m,a}$ (J/g)	$\Delta H_{m,b}$ (J/g)	$f_b$
3	-20.53	-16.67	-127.06	0.884
5	-20.88	-19.19	-141.15	0.880
7	-25.48	-7.88	-53.99	0.872
9	-27.11	-13.83	-64.24	0.823
11	-27.15	-22.59	-61.30	0.731